Whereas O_2 may penetrate only 1 to 2 mm in a nearshore sediment (*23, 24*), sulfate reduction rates are rarely measured in less than 1 cm depth increments. High near-the-surface rates of sulfate reduction as reported in many nearshore sediments (*25, 26*), however, allow the possibility that sulfate reduction might occur in the aerobic zone. By contrast, in many continental margin sediments, particularly at low sedimentation rates and farther offshore, sulfate reduction is suppressed near the sediment surface and begins only below the zone of O_2 penetration (*24*). In this case, sulfate-reducing bacteria apparently cannot compete with other bacterial populations, such as iron-reducing bacteria (*27*), for organic substrate, although the details of these competitive interactions are not well known.

REFERENCES AND NOTES

1. B. B. Jørgensen, *Nature* **296**, 643 (1982); D. E. Canfield, *Deep-Sea Res.* **36**, 121 (1989).
2. G. W. Skyring, L. A. Chambers, J. Bauld, *Aust. J. Mar. Freshwater Res.* **34**, 359 (1983).
3. P. N. Froelich *et al.*, *Geochim. Cosmochim. Acta* **43**, 1075 (1979); R. A. Berner, *Early Diagenesis* (Princeton Univ. Press, Princeton, NJ, 1980).
4. D. J. Des Marais *et al.*, in *Microbial Mats: Physiological Ecology of Benthic Microbial Communities*, Y. Cohen and E. Rosenberg, Eds. (American Association for Microbiology, Washington, DC, 1989), chap. 17.
5. B. B. Jørgensen, Y. Cohen, D. J. Des Marais, *Appl. Environ. Microbiol.* **53**, 879 (1987).
6. B. B. Jørgensen and D. J. Des Marais, *Limnol. Oceanogr.* **33**, 99 (1988).
7. _____ *FEMS (Fed. Eur. Microbiol. Soc.) Microbiol. Ecol.* **38**, 179 (1986).
8. R. S. Oremland and D. G. Capone, in *Advances in Microbial Ecology*, K. C. Marshall, Ed. (Plenum, New York, 1988), vol. 10, pp. 285–383. To evaluate molybdate inhibition, we equilibrated a section of mat in the light for 2 hours in pond water amended to 60 mM molybdate (pond water sulfate is about 90 mM). A separate piece of mat was treated in an identical manner but without molybdate. The depth distribution of O_2 and primary production were similar in both mats just before injection with ^{35}S-labeled SO_4^{2-} and did not change during the time course of the incubation, which was in the light.
9. J. R. Postgate, *The Sulfate Reducing Bacteria* (Cambridge Univ. Press, Cambridge, 1979).
10. B. B. Jørgensen, *Mar. Biol.* **41**, 7 (1977).
11. H. D. Peck, Jr., and T. Lissolo, in *The Nitrogen and Sulfur Cycles*, J. A. Cole and S. J. Ferguson, Eds. (Cambridge Univ. Press, Cambridge, 1988), pp. 99–132.
12. D. E. Canfield *et al.*, *Chem. Geol.* **54**, 149 (1986).
13. I. R. Kaplan and S. C. Rittenberg, *J. Gen. Microbiol.* **34**, 195 (1964). Isotopic measurements were made on mat used for the 30°C daytime experiment (Fig. 3). Mat was sectioned and frozen at about 1700 hours. Reduced sulfur was collected by chromium reduction (*12*), and isotopic analysis was performed on a VG SIRA 10, gas-source mass spectrometer.
14. C. V. Dijk, A. van Berkel-Arts, C. Veeger, *FEBS (Fed. Eur. Biochem. Soc.) Lett.* **156**, 340 (1983).
15. J. A. Hardy and W. A. Hamilton, *Curr. Microbiol.* **6**, 259 (1981); H. Cypionka, F. Widdel, N. Pfennig, *FEMS (Fed. Eur. Microbiol. Soc.) Microbiol. Ecol.* **31**, 39 (1985); W. Dilling and H. Cypionka, *FEMS (Fed. Eur. Microbiol. Soc.) Lett.* **71**, 123 (1990).
16. Based on unpublished observations made with O_2 microsensors.
17. B. B. Jørgensen, *Limnol. Oceanogr.* **22**, 814 (1977).
18. Y. Cohen, *Eos* **65**, 905 (1984).
19. N. P. Revsbech, B. B. Jørgensen, T. H. Blackburn, Y. Cohen, *Limnol. Oceanogr.* **28**, 1062 (1983).
20. D. Hastings and S. Emerson, *ibid.* **33**, 391 (1988).
21. D. E. Canfield, unpublished sulfate reduction rate measurements.
22. B. Hargrave, personal communication.
23. N. P. Revsbech, J. Sørensen, T. H. Blackburn, J. P. Lomholt, *Limnol. Oceanogr.* **25**, 403 (1980).
24. B. B. Jørgensen and N. P. Revsbech, *Ophelia* **31**, 29 (1989).
25. S. Thode-Andersen and B. B. Jørgensen, *Limnol. Oceanogr.* **34**, 793 (1989).
26. P. M. Crill and C. S. Martens, *Geochim. Cosmochim. Acta* **51**, 1175 (1987).
27. D. R. Lovely and E. J. P. Phillips, *Appl. Environ. Microbiol.* **53**, 2636 (1987).
28. D. J. Des Marais, *Trends Ecol. Evol.* **5**, 140 (1990).
29. N. P. Revsbech, B. B. Jørgensen, O. Brix, *Limnol. Oceanogr.* **26**, 717 (1981); *ibid.* **28**, 749 (1983); N. P. Revsbech, P. B. Christensen, L. P. Nielsen, in *Microbial Mats: Physiological Ecology of Benthic Microbial Communities*, Y. Cohen and E. Rosenberg, Eds. (American Association for Microbiology, Washington, DC, 1989), chap. 13.
30. B. B. Jørgensen, *J. Geomicrobiol.* **1**, 11 (1978).
31. Cores were injected vertically and incubated from 10 to 30 min under ambient conditions of light and temperature. Time course experiments showed that, with these short incubation times, no reduced ^{35}S was reoxidized back to sulfate, even in the aerobic zone, where sulfide was rapidly oxidized to elemental sulfur. Reduced ^{35}S was recovered with the use of a modification of the chromium reduction technique (*12, 32*), in which sulfide is liberated from dissolved sulfide, mineral sulfides, and elemental sulfur, but not organic sulfur compounds (*12*).
32. N. N. Zhabina and I. I. Volkov, in *Environmental Biogeochemistry: Methods, Metals and Assessment*, W. E. Krumbein, Ed. (Ann Arbor Science, Ann Arbor, MI, 1978), pp. 735–745.

33. We thank the Exportadora de Sal for logistical support and for access to their ponds. D.E.C. acknowledges support by the National Research Council. We also acknowledge helpful comments of L. Jahnke, L. Hochstein, and two anonymous reviewers. Work was conducted under a grant (to D.J.D.) from the National Aeronautics and Space Administration Planetary Biology Program. Sulfur isotope analysis supported by Natural Environment Research Council grant GR3-6254 to R. Raiswell (Leeds University, United Kingdom).

24 September 1990; accepted 14 January 1991

Variations in Terrigenous Input into the Deep Equatorial Atlantic During the Past 24,000 Years

ROGER FRANCOIS AND MICHAEL P. BACON

Estimates of terrigenous fluxes at three different water depths at two sites in the equatorial Atlantic by normalization against excess ^{230}Th flux indicate that the flux of terrigenous material to the seafloor was significantly higher during the last glacial period than it is today. Fluxes started to decrease during deglaciation and reached minimal values in the middle of the Holocene. From 15,000 to 5,000 years ago, there was a substantial increase in flux with increasing water depth below 2,800 meters; this increase may reflect resuspension and lateral transport of slope and rise sediment, possibly because of intensification of deepwater circulation during that period.

THE INPUT OF TERRIGENOUS CLAYS into Atlantic deep-sea sediments has fluctuated with time. Clays usually have accumulated at higher rates during periods of low sea-level stand; this trend thus accounts in large part for the low amounts of $CaCO_3$ found in the glacial sections of Atlantic cores (*1–3*). Because of this apparent connection with climatic cycles, knowledge of changes in the mode of terrigenous input into deep-sea sediments is important for understanding the climate perturbations that occurred during the Quaternary.

We investigated variations in terrigenous flux in the equatorial Atlantic during the last 24,000 years by ^{230}Th profiling in six sediment cores taken at different water depths from the slopes of two rises (Sierra Leone Rise and Ceará Rise; Fig. 1). This method is based on observations from sediment trap studies suggesting that the annually averaged fluxes of excess ^{230}Th ($^{230}Th_{ex}$) to the seafloor are nearly constant and close to the expected rates of production from the radioactive decay of ^{234}U dissolved in the overlying water column. Thus, we contend that $^{230}Th_{ex}$ can be used as a reference against which the flux of other sedimentary components can be estimated (*3–6*). In contrast to methods where paleoflux estimates are obtained from average accumulation rates between dated sediment horizons, our method gives a flux estimate at each sampled point and thus allows better time resolution.

The $^{230}Th_{ex}$ mass balance (ψ) for sediments that accumulated in the Holocene and glacial sections of the six cores (Table 1) indicates the extent to which $^{230}Th_{ex}$ was brought to the site by post-depositional redistribution and lateral transport over the integrated periods (*4, 5, 7*). Values close to 1 indicate that the effect of these processes was small and that sediment accumulation at the site was dominated by the downward flux of material from the overlying water column. For these cases, ^{230}Th-normalized fluxes provide good estimates of pelagic settling fluxes. This situation was observed in most of the sections we analyzed. Exceptions were the glacial section of the deepest

Chemistry Department, Woods Hole Oceanographic Institution, Woods Hole, MA 02543.

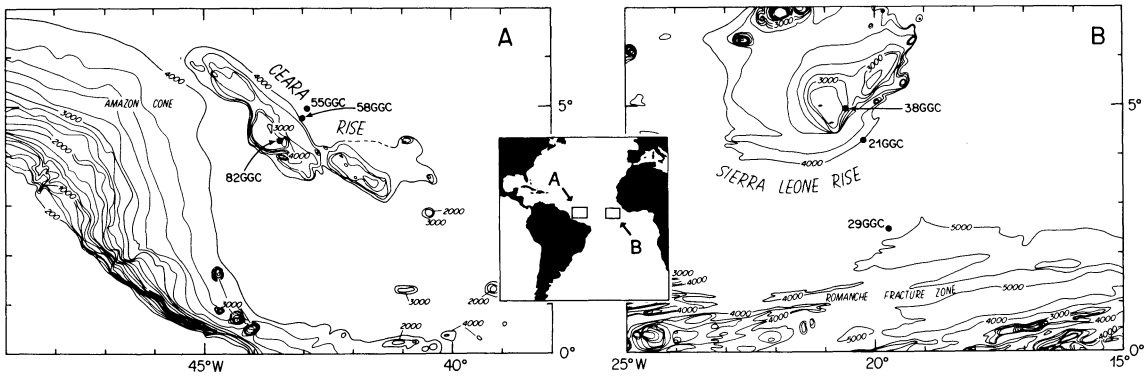

Fig. 1. Study area and core locations. Three cores from different depths were analyzed at each site. (**A**) Ceará Rise: KNR110 82GGC (2816 m); KNR110 58GGC (4341 m); KNR110 55GGC (4556 m). (**B**) Sierra Leone Rise: EN066 38GGC (2931 m); EN066 21GGC (3995 m); EN066 29GGC (5104 m).

Table 1. $^{230}Th_{ex}$ mass balance (ψ) for sediments that accumulated during Stage (Stg) 1 and Stage 2 at different water depths on Ceará Rise and Sierra Leone Rise. A value of ψ = 1 indicates exact balance with production of ^{230}Th in the water column.

Core	Water depth (m)	ψ Stg 1	ψ Stg 2
Ceará Rise			
KNR110 82GGC	2816	1.02	1.77
KNR110 58GGC	4341	0.81	1.26
KNR110 55GGC	4556	0.92	1.10
Sierra Leone Rise			
EN066 38GGC	2931	0.96	0.99
EN066 21GGC	3995	1.15	0.95
EN066 29GGC	5104	1.12	1.82

core from Sierra Leone Rise (EN066 29GGC) and that of the shallowest core from Ceará Rise; in both cases ψ was significantly greater than 1 (Table 1). For core EN066 29GGC, additional $^{230}Th_{ex}$ was probably brought by downslope transport, and normalized fluxes are still good approximations of the actual pelagic settling fluxes (*5*). The large ψ obtained for the glacial section of KNR110 82GGC (and to a lesser extent for KNR110 58GGC) likely reflects resuspension and lateral transport of fine materials from the prograding sedimentary cone of the Amazon River during low sea-level stand (*8*). Mass balance calculations for ^{14}C-dated intervals in this core reveal that ψ was significantly greater than 1 only in sediments deposited before 14 ka (thousand years ago) (*5*). The terrigenous fluxes estimated from the older part of this core might thus be somewhat overestimated, although the error appears to be relatively minor (*5*).

Normalized terrigenous fluxes at both sites are high in the part of the core corresponding to isotope Stage 2 (Fig. 2) and decrease at the early stage of deglaciation (*9*). They reach a minimum (~0.2 g cm^{-2} per 1000 years) in the mid-Holocene part of the core and increase slightly in the last 5000 years of the core. They are consistently higher in the cores from the western equatorial Atlantic. Average terrigenous flux during Stage 2 on Ceará Rise (~1.3 g cm^{-2} per 1000 years) is about twice that recorded on Sierra Leone Rise (0.6 g cm^{-2} per 1000 years).

The high input of terrigenous materials into the deep sea during Stage 2 most likely indicates that when sea level was low, rivers flowed across the continental shelves, which were above sea level, and discharged their load directly into deep water (*10*). High erosion rates in the glaciated northern latitudes must have also increased the load of many rivers fed directly by glaciers, whereas at low latitude, intensification of the trade winds (*11*) and more arid conditions in western tropical Africa (*12*) resulted in large amounts of eolian transport.

The lack of increasing trend with water depth in the terrigenous flux recorded during the glacial period suggests that the mode of addition of terrigenous material into the deep sea was dominated by direct input into the upper water column (that is, at depths shallower than 2800 m). Resuspension and lateral advection from the continental slope and rise, at depths below 2800 m, were evidently insignificant. Most of the fluvial load was probably deposited on the adjacent continental slopes, but some fine material must have been transported laterally by currents in the upper water column. Sinking of this material, along with eolian dust, can account for the high and nearly constant terrigenous flux with depth below 2800 m (Fig. 3A). The higher fluxes found in the western Atlantic could reflect the relative proximity of the Amazon River, which is known to have been an important point source of terrigenous material at that time (*8, 13*). The major rivers draining into the eastern Atlantic (Senegal, Niger, and Zaire) supply comparatively little material (*14*) and are more distant from the nearest cores.

Significant excess accumulation of $^{230}Th_{ex}$ ($\psi >> 1$) occurred in the glacial section of the core taken from the top of Ceará Rise (KNR110 82GGC). This value indicates that the sediment was focused at this site, presumably by turbidite resuspension from the Amazon cone and lateral advection (*5*). Because ψ decreases with depth (Table 1) and is close to 1 in the deepest core (KNR110 55GGC), relatively little sediment from the Amazon cone must have reached the eastern slope of Ceará Rise (Fig. 3A), possibly because of the increasing distance between the deeper sites and the turbidite field.

The data also indicate that the mode of input of terrigenous sediment changed drastically as the sea level rose. Flooding of the continental shelves would have gradually cut off the direct supply of fluvial material into deep water (Fig. 3B). During high sea-level stands, this type of supply is virtually elimi-

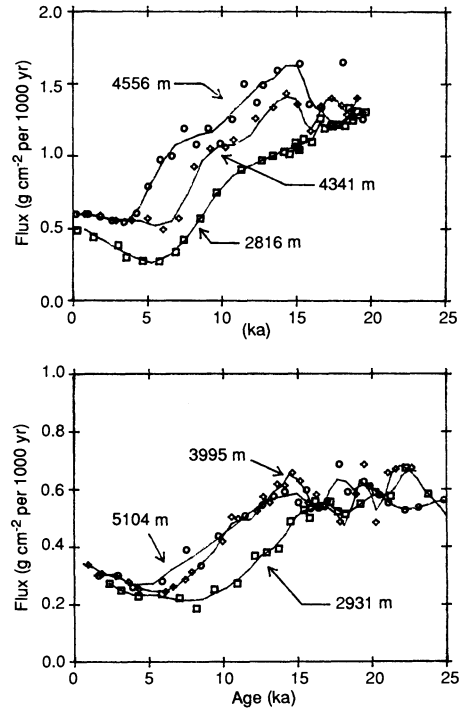

Fig. 2. Normalized terrigenous fluxes on Ceará Rise (**Top**) and Sierra Leone Rise (**Bottom**). Open symbols represent individual data points. The data are listed in (*5*). The smoothed curves were obtained from flux calculations performed at depth intervals of 1 or 2 cm after interpolation from the data with a cubic spline and subsequent smoothing by a least squares procedure.

nated because riverine materials are largely trapped in estuaries or deposited on the inner shelves (*10, 14*). Similarly, the extent of eolian transport is thought to have been significantly curtailed during deglaciation and early Holocene because of a decrease in wind intensity (*11*) and diminished aridity in western Africa (*12*). Under these circumstances, lesser amounts of terrigenous material would have been added directly into the upper water column, as indicated by the gradual decrease in terrigenous fluxes from the onset of deglaciation to the mid-Holocene (Fig. 2).

During that time interval, however, terrigenous fluxes increased gradually with water depth in the cores from the western Atlantic. A similar trend occurred in the eastern Atlantic cores between 2931 and 3995 m, but not deeper (Fig. 2). These differences in flux seem too large to be simply a result of miscorrelation between cores, because relative shifts of ~4000 years would be required. Instead, this pattern of sedimentation suggests that some of the terrigenous material found in these cores during that period was transported laterally at depths below 2800 m. Because a similar pattern is found both in the western and eastern equatorial Atlantic, it can also be argued that the process responsible for this enhanced lateral transport of sediment was a large-scale event and not simply a localized phenomenon. One likely source for this material is resuspension and lateral advection of slope and rise sediment by western boundary undercurrents. Because bottom nepheloid layers appear to be produced by accelerated abyssal currents (*15*), larger lateral transport of terrigenous sediment could indicate that deepwater circulation became more intense at this time. The more pronounced increase in flux with water depth observed below 4000 m in the western Atlantic compared to the eastern Atlantic (Fig. 2) is consistent with a source at the western boundary and eastward transport of sediment in a pattern similar to that of present-day nepheloid transport (*15, 16*). The lack of an increase in terrigenous flux below 4000 m in the eastern Atlantic may reflect blocking of the eastward transport of suspended solids by the Mid-Atlantic ridge at depth below the level of the Romanche fracture zone [~3750 m (*17*)]. At shallower depths, such transport could have occurred freely; such transport could account for the increase in terrigenous flux in the eastern equatorial Atlantic between 2931 and 3995 m (Fig. 3B).

A brief maximum in the terrigenous flux is evident in the deepest core from Ceará Rise at the onset of deglaciation (Fig. 2). This feature was produced after the data indicate

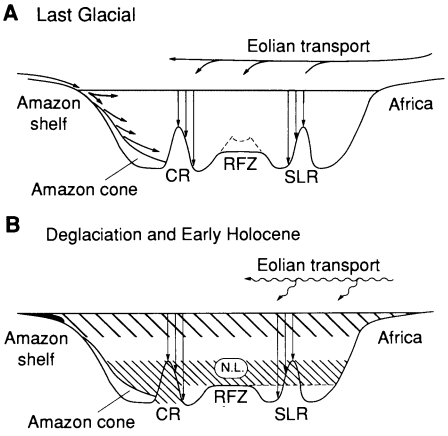

Fig. 3. Mode of terrigenous sediment input to the deep equatorial Atlantic. (**A**) During the last Glacial period; (**B**) during the last deglaciation and early Holocene. Dashed lines in (**A**) show location of the Mid-Atlantic Ridge. RFZ, Romanche Fracture Zone; CR, Ceará Rise; SLR, Sierra Leone Rise; N.L., nepheloid layer produced by western boundary undercurrents.

that lateral transport in the nepheloid layer had become intensified but before direct input of fluvial material was significantly reduced by the rise in sea level. This feature suggests that intensification of deepwater circulation was established before significant sea-level rise.

In the Late Holocene, a small but definite increase in normalized terrigenous flux is observed at both sites (Fig. 2), coinciding with a significant reduction in the increase in terrigenous flux with depth. A similarly small increase in terrigenous flux with depth (0.12 g cm^{-2} per 1000 years between 3755 and 5068 m) was also measured with sediment traps deployed in nearby Demerara Abyssal Plain (*18*). This pattern indicates that the intensity of nepheloid-layer transport below 2800 m decreased and possibly that the intensity of deepwater circulation was reduced during the last 5000 years. The small increase in normalized terrigenous flux observed at that time must, therefore, result from higher input to the upper ocean above 2800 m. The source of this material may be from either higher eolian transport from an increasingly dry African continent (*11, 12*) or a renewed direct supply of fluvial material, possibly as estuaries and other areas on the inner shelves became overloaded with sediments and as prograding shorelines allowed more sediment to be transported offshore.

The contrasting depth gradient in terrigenous flux during Stage 2 and Late Holocene with that of the transition period, observed at both sides of the equatorial Atlantic, suggests therefore that deepwater circulation was more intense during deglaciation and, as a result, that a more dynamic sedimentary environment was produced in the deep sea. The conditions continued for approximately 10,000 years before the oceans reverted to more quiescent conditions about 5,000 years ago (*19*).

REFERENCES AND NOTES

1. W. F. Ruddiman, *Geol. Soc. Am. Bull.* **82**, 283 (1971).
2. W. B. Curry and G. P. Lohmann, *Mar. Geol.* **70**, 223 (1986).
3. M. P. Bacon, *Isot. Geosci.* **2**, 97 (1984).
4. D. O. Suman and M. P. Bacon, *Deep-Sea Res.* **36**, 869 (1989).
5. R. Francois, M. P. Bacon, D. O. Suman, *Paleoceanography* **5**, 761 (1990).
6. The normalized terrigenous flux, F_i, is given by $F_i = \beta \cdot z \cdot f_i / {}^{230}Th^{o}_{ex}$; where f_i is the terrigenous weight fraction in sediment [because opal concentrations were small (*5*), terrigenous sedimentary fractions were taken as equivalent to the noncarbonate fractions], ${}^{230}Th^{0}_{ex}$ is the activity of excess ${}^{230}Th$ (decay-corrected to time of deposition, based on $\delta^{18}O$ stratigraphy and ${}^{14}C$ dates), β is the production rate of ${}^{230}Th$ from ${}^{234}U$ in the overlying water column (2.63×10^{-5} dpm per cubic centimeter per thousand years), and z is the water depth.
7. ψ is given by

$$\psi = \left(\int_{r_1}^{r_2} [{}^{230}Th^{o}_{ex}] \rho_b \, dr \right) / \beta_z \, (t_1 - t_2)$$

where $[{}^{230}Th^{o}_{ex}]$ is the excess ${}^{230}Th$ concentration (decay corrected to the time of deposition) in sediment, ρ_b is the dry bulk density of the sediment, r_1 and r_2 are the depths of the boundaries between the isotopic stages, and t_1 and t_2 are the corresponding dates.
8. J. E. Damuth, *Geol. Soc. Am. Bull.* **88**, 695 (1977).
9. The time scales are based on $\delta^{18}O$ stratigraphy [(*2*); W. B. Curry and G. P. Lohmann, *Paleoceanography* **5**, 487 (1990)] and on ${}^{14}C$ accelerator mass spectrometry (AMS) dates available for core KNR110 82GGC [W. S. Broecker *et al.*, *Paleoceanography* **3**, 509 (1988)]. Dates were assigned by linear interpolation with four points of reference: core top, present; mid-deglaciation point, 12.1 ka; onset of deglaciation, 14.9 ka; Stage 2/3 boundary, 24 ka. Ages for the onset of deglaciation and mid-deglaciation were chosen so as to fit the AMS ${}^{14}C$ dates of KNR110 82GGC. These dates have not been corrected for reservoir effect and do not incorporate the time-scale corrections suggested by E. Bard *et al.*, *Nature* **345**, 405 (1990). Possible error in the correlation between cores during deglaciation and early Holocene should not exceed 2000 years (*5*).
10. J. D. Milliman, *An. Acad. Bras. Cienc. (Supl.)* **48**, 199 (1976).
11. T. N. Parkin, *Proc. R. Soc. London Ser. A* **337**, 73 (1974); M. Sarnthein and B. Koopmann, *Palaeoecol. Afr.* **12**, 239 (1980); M. Sarnthein, G. Tetzlaff, B. Koopmann, K. Wolter, U. Pflaumann, *Nature* **293**, 193 (1981).
12. L. Pastouret, H. Chamley, G. Delibrias, J.-C. Duplessy, J. Thiede, *Oceanol. Acta* **1**, 217 (1978); E. M. Pokras, *Paleoceanography* **2**, 273 (1987); F. A. Street-Perrott and R. A. Perrott, *Nature* **343**, 607 (1990).
13. J. D. Milliman, C. P. Summerhayes, H. P. Barreto, *Geol. Soc. Am. Bull.* **86**, 610 (1975).
14. J. D. Milliman and R. H. Meade, *J. Geol.* **91**, 1 (1983).
15. I. N. McCave, *Neth. J. Sea Res.* **20**, 167 (1986).
16. P. E. Biscaye and S. L. Eittreim, *Mar. Geol.* **23**, 155 (1977).
17. W. S. Broecker and T. Takahashi, *Deep-Sea Res.* **27A**, 591 (1980).
18. S. Honjo, S. J. Manganini, L. J. Poppe, *Mar. Geol.* **50**, 199 (1982).
19. Haskell *et al.* (*Paleoceanography*, in press) reached a similar conclusion from the grain size analysis of the detrital silt fraction of four piston cores from the Blake Outer Ridge. Also, radiocarbon dating of planktonic and benthic foraminifera in a core from the equatorial Pacific suggests that the deepwater ventilation rate increased rapidly at the beginning of deglaciation [N. J. Shackleton *et al.*, *Nature* **335**,

708 (1988)]. The general agreement between these independent approaches, conducted at different sites, further supports the interpretation of our data.
20. We thank W. B. Curry for providing samples and prepublication stable isotope data, and J. D. Milliman and G. A. Jones for careful and constructive reviews. Funding for this research was provided by the National Science Foundation (grants OCE88-00620 and OCE89-22707). This is Woods Hole Oceanographic Contribution No. 7486.

18 September 1990; accepted 4 January 1991

Repression of HIV-1 Transcription by a Cellular Protein

HIROYUKI KATO, MASAMI HORIKOSHI, ROBERT G. ROEDER*

A cellular DNA binding protein, LBP-1, sequentially interacts in a concentration-dependent manner with two sites that surround the transcriptional initiation site of the human immunodeficiency virus type 1 (HIV-1) promoter. Although sequences in the downstream site (site I) were found to enhance transcription, purified LBP-1 specifically repressed transcription in vitro by binding to the upstream site (site II), which overlaps the TATA element. The binding of human TATA binding factor (TFIID) to the promoter before LBP-1 blocked repression, suggesting that repression resulted from an inhibition of TFIID binding to the TATA element. Furthermore, mutations that eliminated binding to site II both prevented repression in vitro and increased HIV-1 transcription in stably transformed cells. These findings suggest that a cellular factor regulates HIV-1 transcription in a manner that is characteristic of bacterial repressors and that this factor could be important in HIV-1 latency.

TRANSCRIPTIONAL REGULATION OF HIV-1 appears to be intimately related to the onset of acquired immunodeficiency syndrome (AIDS). In addition to the HIV-1–encoded Tat protein (*1*), a number of heterologous viral proteins and extracellular stimuli activate HIV-1 gene expression through multiple cis-acting elements (*2*). However, little is known about negative regulation of HIV-1 transcription (*2*). A cellular protein, termed UBP-1 (*3, 4*) or LBP-1 (*5*), has been described that interacts with a long stretch of the HIV-1 promoter that includes a functional TATA element (*5, 6*) and a potential initiator element (*7*). Deoxyribonuclease I (DNase I) footprint experiments showed that the LBP-1 binding site on the HIV-1 promoter consists of a high-affinity site [site I; nucleotides (nt) −16 to +27] and a low-affinity site (site II; nt −38 to −16) (*4, 5*) (Fig. 1A). Because the TATA-binding transcription initiation factor TFIID has the potential to interact both with the TATA element and with sequences surrounding and downstream of the initiation site (*8, 9*), LBP-1 might also contribute to the regulation of HIV-1 transcription. Mutational analyses have shown that sequences immediately downstream of the initiation site are essential for LBP-1 binding and increase transcriptional efficiency in vitro (*5, 10*).

To directly examine the function of LBP-1, we purified the protein to near homogeneity from a nuclear extract of cultured human cells by chromatography on Bio-Rex 70 and DEAE-Sephacel and by three cycles of oligonucleotide-affinity chromatography (*4, 11*). Comparable binding activities and indistinguishable binding specificities were observed with nuclear extracts from HeLa and Jurkat T cells. On analysis by SDS–polyacrylamide gel electrophoresis and silver staining, the purified protein showed two closely spaced bands of ~64 and 68 kD (*4*) (Fig. 1B, lane 1).

At high molar ratios of factor to template (>14), LBP-1 covered both site I and site II, whereas at lower ratios (<4.5), interactions were observed only with site I (Fig. 1C). To analyze the effects of LBP-1 on transcriptional activity through interactions at these binding sites, we constructed clustered base-substituted mutants (IS1 to IS4) (Fig. 1A). In agreement with previous studies (*5, 12*), a mutant (IS4) with three discontinuous substitutions (nt −3 to −1, +8 to +10, and +16 to +18) in presumptive LBP-1 recognition sites (*3, 4, 5, 12*) completely lost the ability to bind LBP-1 (Fig. 1D, lane 10). Base changes in positions −37 to −32 (IS1 mutant) or −10 to −6 (IS3 mutant) eliminated the extended protection on site II, but mutations in positions −28 to −26 (IS2 mutant, which contains a disrupted TATA element) did not (Fig. 1D, lanes 4, 8, and 6, respectively). These data show that several specific sequences surrounding the HIV-1 TATA element jointly participate, along with site I, in the specific binding of LBP-1 to site II (*13*). Gel mobility shift analysis with DNA fragments extending from nt −42 to +2 and from −6 to +19 suggested that these regions have independent LBP-1 binding activity (*14*), although it remains possible that there are cooperative interactions between these two sites.

The binding specificity of LBP-1 suggests that this factor could regulate HIV-1 transcription, positively or negatively, by direct interplay with basic transcription factors such as TFIID. To test this possibility, we incubated specific mutant templates in a nuclear extract with increasing amounts of purified LBP-1 (Fig. 2A). Transcription from the wild-type template was specifically decreased (by a factor of 100 at the highest factor to template ratio), in good agreement with the quantitative footprint patterns (compare Fig. 1C and Fig. 2A). By contrast, only weak repression, if any, was observed for the mutant template IS3, which shows only site I binding. Similarly, no repression (but rather a slight activation) was observed for IS4, which lacks binding at both sites I and II (*15*). (Although the activation mechanism of the IS4 template by LBP-1 is not known, it could reflect the copurification with LBP-1 of one or more proteins that activate through downstream sequences.) The activity of the adenovirus major late promoter template (pMLcat) was not affected by LBP-1. Thus, it was possible that inhibition of TFIID interactions with the TATA element was a major determinant for the repression mediated by LBP-1. The recent cloning of the human TFIID cDNA (*16*) enabled us to test this possibility with a human TFIID protein that had been expressed in *Escherichia coli* and highly purified by conventional chromatography (*17*) (Fig. 1B, lane 2). Incubation of the templates with exogenous TFIID before the addition of LBP-1 blocked the repression (Fig. 2B, lane 3), whereas simultaneous addition of TFIID with LBP-1 did not (Fig. 2B, lane 4). Control reactions without LBP-1 showed no loss of HIV-1 transcription as a result of an initial incubation with TFIID (Fig. 2B, lanes 1 and 2). Because the binding of TFIID to TATA elements is relatively stable (*8, 18*), TFIID must have remained bound over the incubation period despite the challenge by LBP-1. The dominance of LBP-1 in the normal incubation protocol, or when added simultaneously with exogenous TFIID, is probably explained by the rather slow, temperature-dependent binding of TFIID, which contrasts with that of other site-specific binding proteins such as LBP-1 (*8, 18*).

To investigate the relevance of the in vitro repression activity of LBP-1 to in vivo function, we measured expression from a mutant

Laboratory of Biochemistry and Molecular Biology, The Rockefeller University, New York, NY 10021.

*To whom correspondence should be addressed.